

The structure of solid CO₂ in porous Vycor glass

This article has been downloaded from IOPscience. Please scroll down to see the full text article.

1997 J. Phys.: Condens. Matter 9 7317

(<http://iopscience.iop.org/0953-8984/9/35/007>)

View [the table of contents for this issue](#), or go to the [journal homepage](#) for more

Download details:

IP Address: 171.66.16.209

The article was downloaded on 14/05/2010 at 10:24

Please note that [terms and conditions apply](#).

The structure of solid CO₂ in porous Vycor glass

D W Brown†, P E Sokol†, A P Clarke‡, M A Alam‡ and W J Nuttall§

† Department of Physics, The Pennsylvania State University, University Park, PA 16802, USA

‡ H H Wills Physics Laboratory, University of Bristol, Tyndall Avenue, Bristol BS8 1TL, UK

§ School of Physics and Space Research, Birmingham University, Birmingham B15 2TT, UK

Received 12 June 1997

Abstract. The structure of solid CO₂ confined in porous Vycor glass has been studied as a function of temperature via x-ray diffraction. The confined solid has the same structure as the bulk solid but with a slightly larger lattice constant of 5.644 Å at 150 K compared to the bulk lattice constant of 5.624 Å at the same temperature. Broad diffraction peaks are observed indicating that the solid phase of the CO₂ in the pores forms in small crystallites approximately 160 Å in diameter. This is comparable to the pore dimensions in the Vycor indicating that solidification occurs separately in each of the pores. A large temperature-independent static disorder, analogous to the Debye–Waller factor, was observed in the form of strong damping of the Bragg peaks with increasing Q .

1. Introduction

The properties of gases, liquids, and solids can be altered considerably by confinement in mesoporous materials such as porous Vycor glass, aerogels, and zeolites. These porous media are of great technological interest in fields such as rheology, tribology, and materials engineering. The large surface-area-to-volume ratio of materials adsorbed in porous media provides an opportunity for fundamental studies of the effects of finite size and surface interactions on the phase transitions, structure, and thermodynamic parameters of the adsorbed material.

Studies of gases, liquids, and solids confined in porous media have revealed several interesting properties. For example, gases condense in porous media at pressures below their bulk vapour pressure [1] or above their bulk condensation temperature, in agreement with theoretical predictions [2]. Solidification of confined liquids, however, is suppressed with respect to the bulk freezing temperature [1, 3–5]. Upon solidification the microscopic structure of the confined solid is not necessarily the same as that of the bulk. For example, while Hg in porous Vycor has the same microscopic structure as the bulk [3], H₂O and D₂ in Vycor have different microscopic structures [6, 7]. In some cases, such as for O₂ in xerogel with small pores, the crystalline structure may even be totally eliminated [5].

CO₂ is an excellent candidate to study the effects of confinement since it has been extensively studied both experimentally and theoretically because of its linear shape and strong quadrupolar–quadrupolar interaction. The structure of bulk CO₂ has been known since the early nineteen hundreds [8]. Upon solidification CO₂ enters a $Pa3$ structure which is an fcc lattice with the molecules oriented along the diagonals of the cubic lattice as predicted from minimization of the Gibbs free energy of the solid [9].

Recently the gas–liquid and liquid–solid phase transitions of CO₂ in Vycor glass have been determined through studies utilizing positron annihilation techniques [1] as shown in

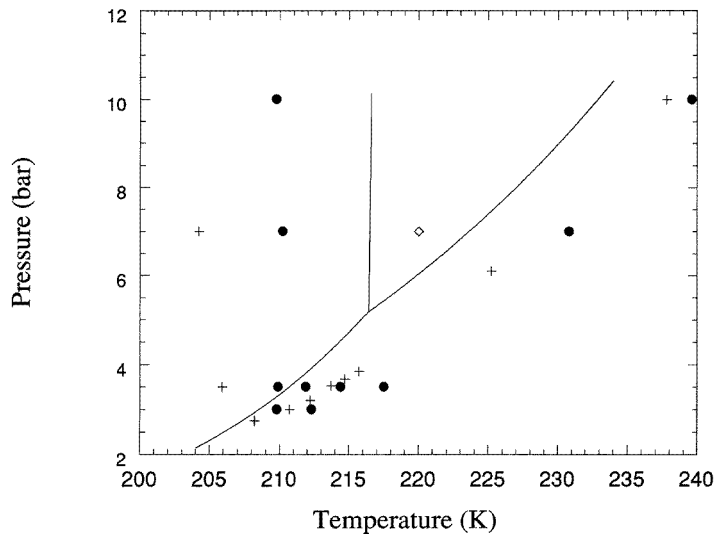


Figure 1. The phase diagram of bulk CO₂ and CO₂ in porous Vycor glass as measured by positron annihilation spectroscopy [1]. The solid lines show the bulk phase transitions. Plus signs represent the phase transitions on the cooling of the confined CO₂ while solid circles represent the phase transitions on the warming of the confined CO₂. The diamond marks the conditions under which CO₂ was condensed into the Vycor for this study.

figure 1. The confined CO₂ condensed at a higher temperature and lower pressure than in the bulk as expected. Likewise the freezing point of CO₂ was depressed below the bulk value and hysteresis between melting and freezing occurred. For example, at 10 bar the freezing point of the confined CO₂ was 204 K while the melting point was 210 K. In bulk CO₂ the freezing and melting point occur concurrently at 216 K [1].

The positron annihilation spectroscopy studies, while providing information on the location of the phase transitions, do not provide any information on the microscopic structure of the confined solid phase. We report studies of the microscopic structure of solid CO₂ adsorbed in porous Vycor glass. Our studies, which were carried out using x-ray diffraction, find that the CO₂ solidifies into crystallites with average dimensions of 160 Å, with a structure which is consistent with the *Pa3* structure of bulk solid CO₂. However, the unit-cell size for the confined solid is larger than what has been observed in the bulk at the same temperature indicating a less dense solid in the pores. Also a significant amount of disorder is observed in the arrangement of the molecules which cannot be accounted for with the Debye–Waller effect.

2. Experimental details

The confining medium used in these studies was porous Vycor glass. Vycor is produced by spinodal decomposition of a boro-silicate glass followed by leaching of the boron-rich phase, and has been extensively characterized [10]. The sample used in this measurement was in the form of a disk with a diameter of 14 mm and a thickness of 1.5 mm. The nominal pore diameter of the Vycor was 70 Å. The sample was cleaned by boiling in a 30% hydrogen peroxide solution. The sample was then rinsed in acetone, isopropyl alcohol, and distilled water, and this was followed by drying at an elevated temperature in a dry

nitrogen atmosphere. The clean Vycor was then transferred to a tightly fitting cell, designed to minimize free volume. Beryllium windows were utilized to allow the passage of x-rays. The cell was mounted on a closed-cycle refrigerator (CCR), and the temperature was monitored with a silicon diode thermometer.

The x-ray scattering measurements were performed at beamline 2.3 at the Synchrotron Radiation Source, Daresbury Laboratory. Beamline 2.3 is optimized for powder diffraction studies. The incident beam was not focused and had a height of 0.5 mm and a wavelength of 1.1990 Å as determined from a standard silicon sample. The detector slits were a distance of 750 mm from the sample and were opened 2 mm yielding an approximate angular acceptance of 0.15°. Transmission geometry was used with the incident beam normal to the face of the Vycor disk and the detector rotating in the vertical plane. The weight of the CCR dictated that the sample not be rotated more than a few degrees, but rather be kept vertical throughout the measurement. Diffraction peaks from the Be windows were used to calibrate the instrument as well as providing a measure of the instrumental resolution.

CO₂ was loaded into the sample cell at 220 K and 7 bar, in the bulk liquid phase. A small decrease in the x-ray transmission through the cell was observed as the CO₂ condensed into the pores of the Vycor glass. The cell was slowly cooled to 145 K, and measurements were taken at 150 K and 201 K on warming.

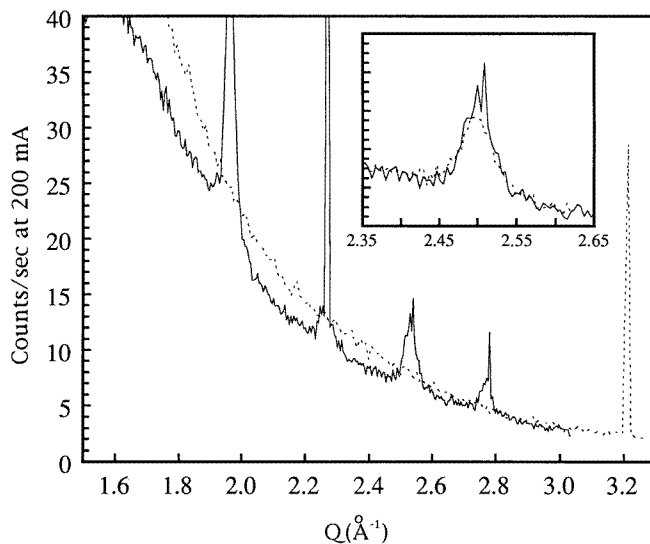


Figure 2. The scattering of the confined liquid (dashed line) and solid (solid line) CO₂, at $T = 220$ and 150 K respectively. The scattering from the Vycor and the cell has not been removed. The inset shows a scattering near the bulk (210) peak before and after a small rotation, of the cell. Note the disappearance of the sharp peak on rotation, and the slight offset of the sharp peak to higher Q .

3. Results

The observed scattering from CO₂ in Vycor in both the solid and liquid phases is shown in figure 2. The scattering consists of contributions from the confined CO₂, the confining Vycor, and the Be windows in the beam path. The data have been corrected for attenuation

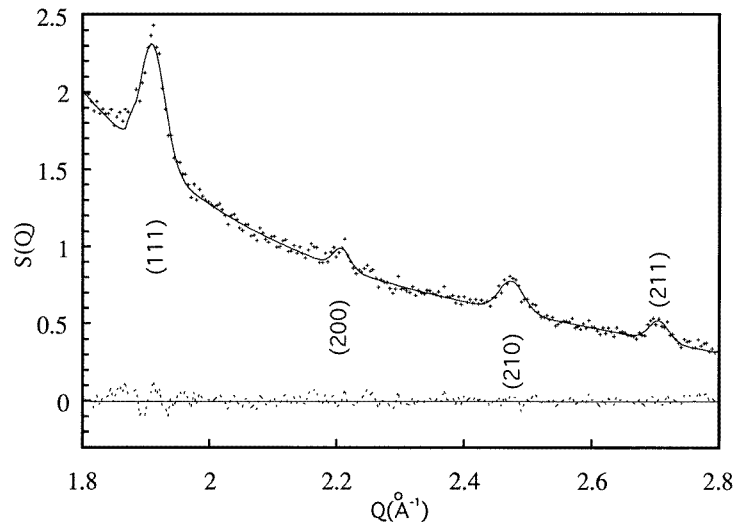


Figure 3. The scattering of the confined solid (upper data points) with the cell oriented to remove the contribution of bulk CO₂. Contributions due to the sample and Vycor have not been removed. The solid line represents the fit to the data, and the lower dashed curve is the residue.

of the x-ray beam due to absorption by the Vycor and CO₂. As can be seen, the scattering in the liquid phase shows only a single sharp feature at $Q = 3.2 \text{ \AA}^{-1}$ due to the Be windows. The scattering from the short-range order of the glassy Vycor and liquid CO₂ contribute only a monotonically decreasing smooth background for the range of momentum transfer covered.

Upon cooling to low temperature, diffraction peaks appear, as can be seen in figure 2. These diffraction peaks are a clear indication that some fraction of the CO₂ develops crystalline ordering on freezing. The peaks that appear can be separated into narrow peaks, which have a width determined by the instrumental resolution, and broad peaks, which have a width that is an order of magnitude larger than the instrumental resolution. These peaks are nearly coincident in their locations. However, small rotations of the sample, $\theta = \pm 1^\circ$, brought on the disappearance of the sharp peaks while the broad peaks remained unchanged. The inset of figure 2 shows a blow up of the area surrounding the bulk (210) peak before and after a small rotation, of the sample. Along with the disappearance of the sharp peak after the rotation, note that the sharp peak is located at slightly higher Q than the broad peak.

We believe that the narrow peaks are due to polycrystallites of CO₂ that have formed on the external surface of the Vycor while the broad peaks are due to CO₂ within the pores. Due to the pressure at which the cell was loaded there was necessarily some bulk CO₂ surrounding the cell when the cell decreased below the bulk freezing point. It is likely that the bulk CO₂ would crystallize into a polycrystalline sample. The disappearance of the narrow peaks with small sample rotations is characteristic of polycrystallites.

The broad peaks, however, were independent of rotation of the sample indicating a powder sample. Since crystallites forming within the randomly oriented pores of the Vycor would mirror these random orientations we believe that these peaks must be due to CO₂ adsorbed into the pores of the Vycor. The broad peaks disappeared on warming between 208 K and 211 K, well below the bulk melting point and in agreement with the phase

diagram of Duffy *et al* [1], confirming that the broad peaks were due to crystalline CO₂ within the porous network.

The scattering from solid CO₂ in the pores of the Vycor is shown in figure 3. The scattering consists of four broad diffraction peaks over a smooth background. The sharp peaks due to bulk single crystallites outside the Vycor are of little interest, and have been eliminated by appropriately orienting the sample. The four observed peaks are not sufficient to uniquely determine the crystallographic structure of the confined solid. However, we may use these observed peaks to compare to the structure of the bulk solid.

Table 1. Position and intensity parameters of the peaks due to the confined solid at 150 K obtained from Gaussian fits. The measured bulk positions and calculated bulk positions and intensities are also listed. Uncertainties of the confined positions are estimated to be $\pm 0.003 \text{ \AA}$. Peaks are indexed assuming $Pa3$ structure.

Reflection	Position, confined (\AA^{-1})	Position, bulk (\AA^{-1})	Position, calculated (\AA^{-1})	Intensity, confined	Intensity, perfect crystal
111	1.923	1.933	1.935	1.00	1.000
200	2.224	2.238	2.234	0.08	0.150
210	2.486	2.497	2.498	0.32	0.580
211	2.722	2.735	2.736	0.11	0.458

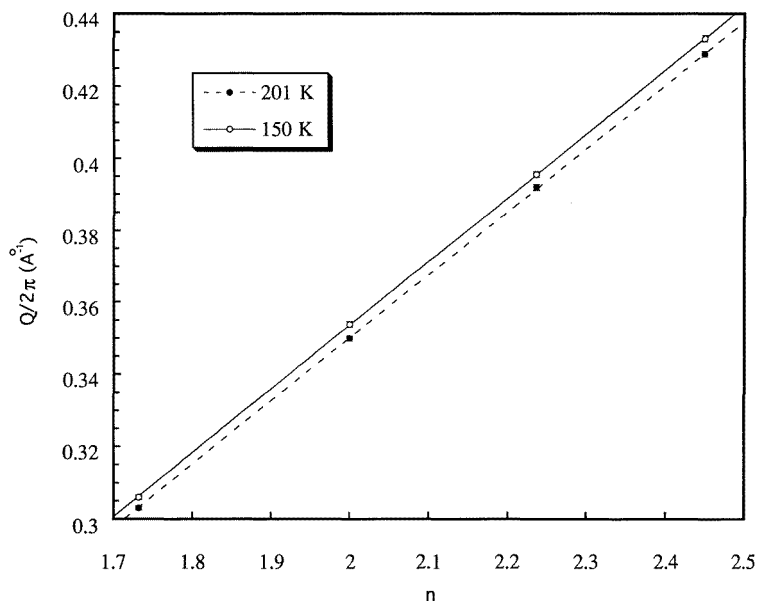


Figure 4. A plot of the location of the diffraction peaks in units of $\text{\AA}^{-1}/2\pi$ versus $n = \sqrt{h^2 + k^2 + l^2}$ at $T = 201$ and 150 K. The lattice constant is given by the inverse of the slope of the fitted line.

The locations of the broad peaks due to the crystalline CO₂ in the pores have been obtained by fitting each peak to a Gaussian form plus a smooth background. The results of these fits, which were carried out simultaneously for all four observed peaks, are also shown in figure 3. The locations of the peaks at 150 K are shown in table 1. Also included

in the table are the locations of the diffraction peaks from the bulk solid, obtained from different orientations of the sample, at the same temperatures. As can be seen in the table, the location of the sharp (bulk) peaks is in good agreement with the predicted locations based on the accepted lattice constant of $a = 5.624 \text{ \AA}$ at 150 K [11]. The locations of the broad peaks, however, are consistently lower in Q -space than the bulk peaks. The close correspondence between the location of the bulk and confined peaks suggests that the confined solid may have the same structure. In that case we can easily index the observed peaks shown in figure 3. Assuming the same structure as the bulk, the reflections that we observe are (111), (200), (210), and (211). For the cubic structure observed in the bulk, the location of the Bragg peak in reciprocal space is given by $Q = (2\pi/a)\sqrt{h^2 + k^2 + l^2}$ where $Q = 2\pi/d$ is the reciprocal-lattice vector for the reflection, and h , k , and l are the Miller indices of the reflection. Figure 4 shows the locations of the peaks versus $\sqrt{h^2 + k^2 + l^2}$ where h , k , and l have taken the allowed values of the $Pa3$ structure. As can be seen in the figure, the data fall nicely on a straight line, consistent with the assumption that the structure is $Pa3$, as in the bulk. The lattice constant, obtained from the straight-line fits in figure 4, is $5.644 \pm 0.007 \text{ \AA}$ at 150 K and $5.710 \pm 0.007 \text{ \AA}$ at 201 K. This is 0.36% larger than the bulk value of 5.624 \AA at 150 K corresponding to a decrease in the density of the confined solid with respect to the bulk solid.

The intensities of the diffraction peaks provide information both on the spatial arrangement within the unit cell, and the thermal motion and disorder of the atoms about the lattice sites. Assuming that the structure of the confined solid is $Pa3$, as in the bulk, we can extract information on the disorder of the confined solid from the Q -dependence of these intensities. The intensities of the observed diffraction peaks for the confined solid in the pores are shown in table 1. The intensity of the (111) peak has been normalized to unity. Also shown are the intensities for the $Pa3$ structure of bulk CO_2 assuming no transitional or thermal disorder (i.e. a perfect crystal). As can be seen, the intensities of the peaks due to the confined CO_2 decrease more rapidly with increasing Q . This Q -dependence of the intensities of the Bragg peaks is normally associated with thermal motion of the atoms about the lattice sites, and is described by the Debye–Waller factor. However, as we show in the next section, thermal motions alone are insufficient to account for the strong damping that we observe.

The Bragg peaks from the confined CO_2 are much broader than the instrumental resolution. The full width at half-maximum, Γ , of the peaks obtained from the Gaussian fits were Q -independent and were 0.042 and 0.037 \AA^{-1} at 150 and 201 K respectively. These values are identical within the estimated uncertainty of 20%.

4. Analysis and discussion

Two factors, finite size and strain, can produce the large width of the diffraction peaks observed for the confined CO_2 . Finite size produces a broadening that is independent of Q while strain broadening varies as Q^2 . The width of the confined peaks shows no dependence on Q indicating that the confined crystallites have a finite size but are strain free. We can obtain an approximate value for the size of the peak by assuming that the crystallites are parallelepipeds. In this case the characteristic size of the crystallites is given by [12] $L = 2\pi/\Gamma \approx 160 \text{ \AA}$. Sokol *et al* observed crystallites sizes of 400–700 \AA for O_2 and D_2 in Vycor [13]. This larger crystallite size indicates a greater interconnection of the crystallites among neighbouring pores than is present in solid CO_2 in Vycor. In a study of the structure of Hg in porous silica glass with similar pore structure, Kumzerov *et al* [3] measured a crystallite size of 70 \AA . We believe the difference in size is attributable to the

inevitable underfilling of the Hg and the high surface tension of Hg.

The lack of strain in the crystallite coupled with the large increase of density (decrease in molar volume) of CO₂ on freezing suggests that the CO₂ pulls away from the wall on freezing, leaving a small void between the crystal and the wall. If the confined solid were anchored to the pore walls at all points and had a similar density increase on freezing, then the resultant crystallites would be highly strained. Our results show no evidence of strain. Duffy *et al* [1] appealed to similar reasoning to explain their positron annihilation study.

Our results however do not warrant considering the confined solid to be merely small pieces of the bulk solid. Torchet *et al* [14] observed that CO₂ clusters with diameters of order 160 Å have a lattice parameter 0.35% smaller than that of the bulk. This decrease in lattice constant is attributed to the large surface tension which they estimated must be approximately 600 bar. We however have observed an increase in the lattice constant of 0.36%. An increase in the lattice constant of this magnitude cannot be explained with pressure as it would take a very large, i.e. 600 bar, negative pressure to effect such an increase. We believe the increase in the lattice constant to be caused by the attractive potential of the confining media.

An enhanced lattice constant or reduced density is not the only effect of the confining media. In the previous section the intensities of the Bragg peaks due to the confined CO₂ were shown to fall off much more rapidly in Q than for the perfect crystal (table 1). This decrease in intensity can be interpreted in terms of thermal and static disorder in the crystal [12]. Thermal disorder, i.e. the Debye–Waller factor, arises from assumed harmonic vibrations of the constituent atoms about their lattice positions, and gives a Q -dependence to the intensity of the Bragg peaks of the form $I = I_0 \exp(-Q^2 \langle u^2 \rangle)$ where $\langle u^2 \rangle$ is the mean square atomic displacement of the atoms about the lattice sites. While a report of the mean square atomic displacement, $\langle u^2 \rangle$, of solid CO₂ was not to be found in the literature, similar solids such as O₂ are reported [16] as having $\langle u^2 \rangle = 0.01$ Å². We note that our data have such a Q -dependence but the effect is much stronger than could be generated by conventional thermal oscillations.

An enhanced Debye–Waller factor would be expected of diffraction from very small crystallites. In such small crystallites, approximately 160 Å in diameter in this study, the surface-area-to-volume ratio is huge when compared to those of bulk samples. Molecules on the surface will be subject to a greater degree of thermal motions than will internal molecules. Measurements [14] of $\langle u^2 \rangle$ for CO₂ clusters reflect this increased random motion through an enhanced value of $\langle u^2 \rangle \cong 0.17$ Å² in clusters with diameters of approximately 160 Å. This value is, however, still more than a factor of 2 too small to explain our results. Also the Debye–Waller factor is a strongly temperature-dependent quantity near the Debye temperature, which for CO₂ is 152 K [17]. No such temperature dependence of $\langle u^2 \rangle$ is observed in the present study despite the fact that the Debye temperature of the sample lies within our temperature range.

Static disorder may also contribute to the displacement of the molecules from their bulk equilibrium positions [15]. It is conceivable that the disorder induced by the amorphous substrate may substantially increase $\langle u^2 \rangle$ for the CO₂ molecules. Temporal averaging of randomly varying displacements of the molecules due to thermal motion gives rise to an exponentially decreasing envelope to the diffraction pattern. The random nature of the potential due to the amorphous Vycor substrate could cause random static displacements that when spatially averaged, as in a scattering experiment, place an exponential envelope on the diffraction pattern indistinguishable from that due to thermal motions.

With this in mind we have plotted the observed peak intensity normalized to the expected Bragg intensity of the perfect lattice versus Q^2 on a semilog plot in figure 5. The results are

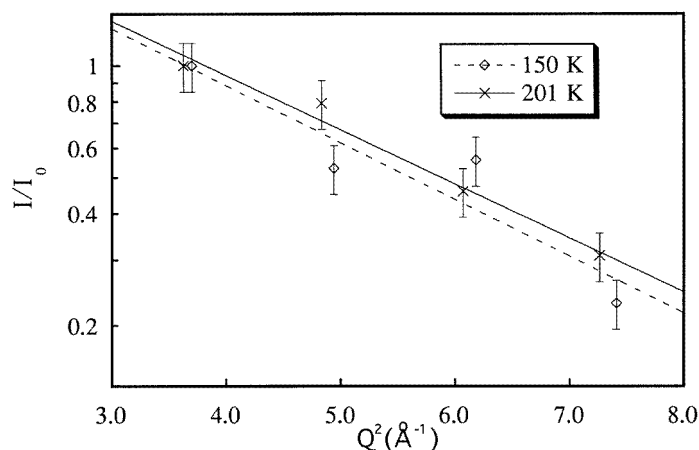


Figure 5. A semilog plot of the ratio of the intensity of the confined solid diffraction peaks (I) to the intensity of the ideal bulk solid diffraction peaks (I_0) versus Q^2 . The intensity of the confined (111) peak has been normalized to the (111) peak of the bulk. The slope of the fitted line is $\langle u^2 \rangle$.

in reasonable agreement with the prediction of a Debye–Waller-like damping of the peak intensity with Q . The slope of the lines yields $\langle u^2 \rangle$ to be 0.35 and 0.33 \AA at 150 and 201 K respectively. These values are the same within our uncertainty. To repeat, the magnitude of the observed mean square atomic displacement as well as the lack of temperature dependence cannot be understood via conventional thermal oscillations but rather is due to static disorder induced by the amorphous porous substrate. Schafer *et al* [18] also measured a large $\langle u^2 \rangle$ in Kr and Xe in silica gels, and also attributed it to static disorder induced by the confining medium.

5. Conclusions

CO₂ solidified within the tortuous pore space of Vycor glass behaves as a very small crystallite suffering from the effects of a random confining potential. The structure of the confined solid is consistent with that of the bulk. Crystallite sizes are of the order of the pore size. An increase in the lattice constant of 0.36% corresponding to a decrease in density of the solid phase as well as large mean square atomic displacements are observed. The large mean square atomic displacement is attributable to static disorder in the system rather than thermal oscillations. We believe these to be manifestations of the confining potential. Further studies with varying pore diameter would be interesting. Also a study of confinement within a crystalline, rather than amorphous, medium with similar pore dimension would shed light on the cause of the large atomic displacements.

Acknowledgments

This work was supported by the National Science Foundation under grant No INT 9600172 and by the American Chemical Society Petroleum Research Fund under grant No 31097-AC5. One of us (MAA) would like to acknowledge the generous support of the EPSRC, UK. We would like to thank M I McMahon, C C Tang, A Neild, and T Rathbone of the

SRS for technical assistance, and W G Stirling of the University of Liverpool for the use of the CCR.

References

- [1] Duffy J A, Wilkinson N J, Fretwell H M and Alam M A 1995 *J. Phys.: Condens. Matter* **7** L27
- [2] Cole M W and Saam W F 1974 *Phys. Rev. Lett.* **32** 985
- [3] Kumzerov Yu A, Nabereznov A A, Vakhrushev S B and Savenko B N 1995 *Phys. Rev. B* **52** 4772
- [4] Awschalom D D, Warnock J and Schafer M W 1986 *Phys. Rev. Lett.* **57** 1607
- [5] Schirato B S, Fang M P, Sokol P E and Komarneni S 1995 *Science* **267** 369
- [6] Bellissent-Funel M-C, Lal J and Bosio L 1993 *J. Chem. Phys.* **98** 4246
- [7] Wang Y, Snow W M and Sokol P E 1995 *J. Low Temp. Phys.* **101** 929
- [8] Keesom W H and Kohler J W L 1934 *Physica* **1** 167
- [9] Kuchta B and Eters R D 1988 *Phys. Rev. B* **38** 6265
- [10] Levitz P, Ehret G, Sinha S K and Drake J M 1991 *J. Chem. Phys.* **95** 6151
- [11] Simon A and Peters K 1980 *Acta Crystallogr. B* **36** 2750
- [12] Warren B E 1990 *X-Ray Diffraction* (New York: Dover)
- [13] Sokol P E, Ma W-J, Herwig K W, Snow W M, Koplík J and Banavar J R 1992 *Appl. Phys. Lett.* **61** 777
- [14] Torchet G, Bouchier H, Farges J, de Feraudy M F and Raoult B 1984 *J. Chem. Phys.* **81** 2137
- [15] Trueblood K N 1992 *Accurate Molecular Structures* ed A Domenicano and I Hargittai (Oxford: Oxford University Press) p 199
- [16] Meier R J and Helmholtz R F 1984 *Phys. Rev. B* **29** 1387
- [17] Manzhelii V G, Tolkachev A M, Bagatskii M I and Voitovich E I 1971 *Phys. Status Solidi b* **44** 39
- [18] Schafer B, Balszunat D, Langel W and Asmussen B 1996 *Mol. Phys.* **89** 1057